Metrol. Meas. Syst. Vol. XVI (2009), No 4, pp. 607-618

PAN POLSKA AKADEMIA NAUK

METROLOGY AND MEASUREMENT SYSTEMS

Index 330930, ISSN 0860-8229

www.metrology.pg.gda.pl

M&MS

MODEL AND LABORATORY SIMULATION OF A INDUCTION MOTOR FOR DIAGNOSTIC PURPOSES

Leon Swędrowski[1)], Jan Rusek[2)]

1) Gdansk University of Technology, Faculty of Electrical and Control Engineering, G. Narutowicza 11/12, 80-952 Gdańsk, Poland (✉ l.swedrowski@ely.pg.gda.pl, +48 59 347 1258)
2) AGH University of Science and Technology, Faculty of Electrical Engineering, Automatics, Computer Science and Electronics, Al. Mickiewicza 30, 30-059 Kraków, Poland (gerusek@cyf-kr.edu.pl)

Abstract

Statistics say that bearings are this part of induction motors which is most susceptible to damage. The equipment employed for bearing diagnostics usually makes use of vibrations as the criterion for technical condition of the bearings. A faulty bearing results in additional motor vibrations. They are reflected in the harmonic content of stator currents. In certain operating conditions the current signal is the sole source of information on the state of the motor. The paper presents a mathematical model of the motor, allowing for rotor eccentricities. Calculated spectra of the stator currents are presented for the cases of operation with rotor vibrations mapping with some approximation the vibrations caused by faulty bearings. The paper presents also the results of laboratory simulations for a motor put into vibrations of adjustable frequency. Vibrations of the motor housing simulate the rotor oscillations caused by a damaged bearing. The results of laboratory simulations permitted to define the relations linking vibrations of the air gap with the components in the stator current spectrum.

Keywords: induction motors, modeling, simulation, current measurement, fault diagnosis.

1. Introduction

The stator current of the motor is distorted in case of appearance of certain type of failures. Under spectral analysis of the motor current one obtains a series of spectrum components which are connected with definite types of damage. An analysis of the amplitudes and phase shifts allows to recognize the type of faults. In comparison with other known methods this one shows certain advantages. Typical faults detected by this method are damages to the stator and rotor windings as well as misalignment of a shaft. The most common cause of failures of squirrel-cage induction motors are, however, failure of bearings.

Damaged elements of a bearing cause radial oscillations of the rotor. This is the source of disturbance in the geometry of the air gap of the machine and, in effect, of modulation of the current [1].

The authors of this paper have made an attempt to create a diagnostic system which would provide credible measurement results, and on their basis, reliable diagnoses.

2. A Mathematical Model of the Motor

In simulation tests on a mathematical model it was assumed that rotor vibrations depend on integral multiples of the rotor's angle of rotation. Let us emphasize that this is only an approximation of actual rotor vibrations which, strictly speaking, generally are not integral multiples of the angle of rotation of the rotor. In the mathematical model we assume that rotor vibrations are perpendicular to the stator axis, *i.e.* – the axes of the rotor and stator remain parallel to each other, also during vibrations of the rotor caused by a damaged bearing. This

Article history: received on Oct. 1, 2009; accepted on Dec. 2, 2009; available online on Dec. 11, 2009.

means that the rotation of the rotor will be similar to the movement of a rotor showing some static eccentricity, which is not constant but vary and is dependent upon the rotor's angular position. Such an approximate comprehension of a damaged bearing facilitated the adaptation of the model of a squirrel-cage induction machine which has been elaborated and originally implemented to diagnostic calculations, taking into account static and dynamic eccentricities as well as slotting.

The implemented calculation model consists of a segment which automatically generated differential equations for linearly independent circuits of the stator and rotor. These circuits include parallel branches of stator phases and external meshes of the rotor squirrel-cage. The equation of one end ring of the squirrel-cage has been also taken into account. The equation of the second end ring is redundant because of the linear dependence on previous ones. The problem lies in the calculation of the matrices of coefficients of self- and mutual inductances: of the stator, rotor and stator-rotor. In the implemented model these coefficients are calculated numerically for several hundred angular positions of the rotor. Each of the coefficients is then developed into a Fourier series. At this stage, derivatives of the inductances with respect to the rotation angle of the rotor are calculated. They are calculated from analytical formulas for the series, with coefficients determined numerically. Derivatives of inductances are used for calculation of the electromagnetic torque present in the mechanical equation [3].

Both the eccentricity and slotting are mapped by lengthening of main magnetic field lines. Thus, slotting results in a reduction of permeance under the slot openings of the stator and rotor. These local reductions of permeance are superimposed on fluctuations of the air-gap permeance due to static and dynamic eccentricities and to vibrations of the rotor with respect to the stator.

As already mentioned, to derive a mathematical model supporting development of diagnostic systems it is indispensable to account for actual winding configuration, eccentricity, rotor vibration and cage asymmetry. The saturation has to be accounted for as well, at least globally via artificial magnification of the air-gap length. To account for actual winding configuration let us assume that the stator contains N_Z coils, placed in N_S slots. These coils are initially assumed to remain separated from one another. Each of these coils can possess individual span and number of turns. The rotor is assumed to possess a single cage which will be described via mesh currents. Each mesh is formed by two adjacent bars, connected by two end-ring segments. The mesh current of one of the end rings constitute one more mesh current which must be accounted for, as it is linearly independent of the others.

Standard Kirchhoff's equations can be written for the above described structure. Equations (1), in matrix or vector form, refer to the stator elementary coils and (2), also in matrix or vector form, refer to rotor-cage meshes. Equation (3) refers to the mesh current of one end ring:

$$\mathbf{V}_S = \mathbf{R}_S\mathbf{i}_S + \frac{d}{dt}\mathbf{L}_S\mathbf{i}_S + \frac{d}{dt}\mathbf{L}_{SR}\mathbf{i}_R, \tag{1}$$

$$\mathbf{0} = \mathbf{R}_R\mathbf{i}_R + \frac{d}{dt}\mathbf{L}_R\mathbf{i}_R + \frac{d}{dt}\mathbf{L}_{RS}\mathbf{i}_S, \tag{2}$$

$$\mathbf{0} = N_R R_{seg} i_{seg} - \mathbf{R}_{seg}\mathbf{i}_R^T + \frac{d}{dt}(N_R L_{seg} + L_{unip}) i_{seg} - \frac{d}{dt}\mathbf{L}_{seg}\mathbf{i}_R^T. \tag{3}$$

The dimensions of the voltage and current vectors $\mathbf{V}_S$ and $\mathbf{i}_S$ are N_Z, where N_Z is the number of stator coils (N_Z = 12). The dimension of the current vector $\mathbf{i}_R$ is N_R, where N_R is the number

of rotor slots (N_R = 22). The row vectors $\mathbf{R}_{seg}$ and $\mathbf{L}_{seg}$ contain N_R values of R_{seg} or L_{seg}, appropriately.

The dimensions of matrices $\mathbf{R}_S$ of stator resistances and $\mathbf{L}_S$ of stator inductances are N_S by N_S.

The dimensions of matrices $\mathbf{R}_R$ of rotor resistances and $\mathbf{L}_R$ of rotor inductances are N_R by N_R.

The dimension of matrix $\mathbf{L}_{SR}$ of stator-rotor inductances is N_S by N_R.

The dimension of matrix $\mathbf{L}_{RS}$ of rotor-stator inductances is N_R by N_S.

R_{seg} and L_{seg} are resistances and leakage inductances of the end ring segments, appropriately.

L_{unip}, the inductance due to the unipolar or shaft flux, was assumed to be zero.

The i_{seg} current is a mesh current of one of the two rotor cage end rings.

The electrical equations (1) through (3) have to be accomplished by two mechanical equations (4) and (5):

$$J\frac{d}{dt}\omega = T_{em} - T_L, \tag{4}$$

$$\frac{d}{dt}\phi = \omega, \tag{5}$$

where:

$$T_{em} = \frac{1}{2}\mathbf{i}_S^T\frac{\partial}{\partial\phi}\mathbf{L}_S\mathbf{i}_S + \mathbf{i}_S^T\frac{\partial}{\partial\phi}\mathbf{L}_{SR}\mathbf{i}_R + \frac{1}{2}\mathbf{i}_R^T\frac{\partial}{\partial\phi}\mathbf{L}_R\mathbf{i}_R. \tag{6}$$

T_L - the loading torque.

The stator elementary coils are first connected to form branches and then configured into phases which, in turn, can be configured into wye (without neutral conductor).

In other words, connection of the stator coils imposes constraints on the currents of the elementary coils: these currents are no longer linearly independent. In fact, the vector $\mathbf{i}_S$ of the elementary currents can be expressed by a smaller number of linearly independent currents, aggregated into vector $\mathbf{I}_S$, making use of the connection matrix $\mathbf{C}$:

$$\mathbf{i}_S = \mathbf{C}\mathbf{I}_S. \tag{7}$$

Matrix $\mathbf{C}$ can only be established by making use of the winding data acquired from the manufacturer.

To account for (7) let us multiply the matrix equation (1) by a transpose of $\mathbf{C}$, that is by $\mathbf{C}^T$:

$$\mathbf{C}^T\mathbf{V}_S = \mathbf{C}^T\mathbf{R}_S\mathbf{C}\mathbf{I}_S + \frac{d}{dt}\mathbf{C}^T\mathbf{L}_S\mathbf{C}\mathbf{I}_S + \frac{d}{dt}\mathbf{C}^T\mathbf{L}_{SR}\mathbf{i}_R$$

or

$$\mathbf{V}_S^{\sim} = \mathbf{R}_S^{\sim}\mathbf{I}_S + \frac{d}{dt}\mathbf{L}_S^{\sim}\mathbf{I}_S + \frac{d}{dt}\mathbf{L}_{SR}^{\sim}\mathbf{i}_R, \tag{8}$$

where:

$$\mathbf{V}_S^{\sim} = \mathbf{C}^T\mathbf{V}_S, \tag{9}$$

$$\mathbf{R}_S^{\sim} = \mathbf{C}^T\mathbf{R}_S\mathbf{C}, \tag{10}$$

$$\mathbf{L}_S^{\sim} = \mathbf{C}^T\mathbf{L}_S\mathbf{C}, \tag{11}$$

$$\mathbf{L}_{SR}^{\sim} = \mathbf{C}^T\mathbf{L}_{SR}. \tag{12}$$

Substitution of (7) into (2) results (after simple manipulations) in:

$$\mathbf{0} = \mathbf{R}_R \mathbf{i}_R + \frac{d}{dt}\mathbf{L}_R \mathbf{i}_R + \frac{d}{dt}\mathbf{L}_{SR}^{\sim T}\mathbf{I}_S. \tag{13}$$

Vector $\mathbf{V}_S^{\sim}$ consists of external phase-to-phase voltages known from supply conditions.

Vector $\mathbf{I}_S$ of linearly independent currents can substitute vector $\mathbf{i}_S$ in formula (6) for electromagnetic torque:

$$T_{em} = \frac{1}{2}(\mathbf{C}\mathbf{I}_S)^T \frac{\partial}{\partial \phi}\mathbf{L}_S \mathbf{C}\mathbf{I}_S + (\mathbf{C}\mathbf{I}_S)^T \frac{\partial}{\partial \phi}\mathbf{L}_{SR}\mathbf{i}_R + \frac{1}{2}\mathbf{i}_R^T \frac{\partial}{\partial \phi}\mathbf{L}_R \mathbf{i}_R$$

or

$$T_{em} = \frac{1}{2}\mathbf{I}_S^T \frac{\partial}{\partial \varphi}\mathbf{L}_S^{\sim}\mathbf{I}_S + \mathbf{I}_S^T \frac{\partial}{\partial \varphi}\mathbf{L}_{SR}^{\sim}\mathbf{i}_R + \frac{1}{2}\mathbf{i}_R^T \frac{\partial}{\partial \varphi}\mathbf{L}_R \mathbf{i}_R. \tag{14}$$

Summarizing, the full set of equations constituting the mathematical model, consists of equations (8), (13), (3), (4), (5) and formula (14).

Equations (9) and (10) are both in vector forms, describe any dynamical state of operation of the cage-rotor induction machine. However, practical use of these equations is conditioned by the knowledge of all the self- and mutual inductances, as well as the derivatives thereof, with respect to rotor angular position φ.

If the inductances of the elementary stator coils were known, then simple multiplication via $\mathbf{C}$ or/and $\mathbf{C}^T$ would result in $\mathbf{L}_S^{\sim}$ or $\mathbf{L}_{SR}^{\sim}$ in equations (8), (13) and formula (14), assumed the connection matrix $\mathbf{C}$ is known from manufacturer's data. This multiplication is implemented in the computer program.

Still, the method must be elaborated, which allowed to calculate all the self- and mutual inductances of the elementary stator coils and separate rotor-cage meshes.

It follows from the well established theory of induction machines that each inductance can be split into the main and leakage parts. The leakage inductance, whether of a stator elementary coil or a rotor-cage mesh, results from the leakage flux, that is from the one not crossing the air gap. In computer implementation of the model discussed, calculation of these inductances is based on classical formulas.

The main inductance (of any elementary circuit) results from the main or working flux, that is that crossing the air gap. This is what remains to concentrate on.

In order to highlight calculations of main inductances, of separate elementary circuits, let us remind that by the assumption of infinitely high iron permeability, the mutual inductance of two coils (of the turns z_1 and z_2) wound on the core of the cross-section S and the air-gap δ, originating from main magnetic flux, is:

$$M_{1,2} = \mu_0 z_1 z_2 \Lambda S, \tag{15}$$

where $\Lambda = 1/\delta$.

By certain assumptions, equivalent formula can be obtain also for the case of an induction machine.

First, let us assume that the envelope of the stator inner surface and that of the rotor outer surface are cylinders with parallel axes. Due to possible eccentricities and damaged bearings, the rotor, at a given time instant can assume an off-centered position.

Let us assume that the lines of the main magnetic flux cross the air gap down the shortest paths between the stator inner and rotor outer surface envelopes. Knowing the geometrical details of eccentricities and damaged bearings, as well as the rotor position φ at the time instant of interest, it is possible to determine the spatial position of the rotor with respect to

the stator bore. This in turn allows to determine the lengths of these paths, for the whole range of (0, 2π) of angular coordinate x (still for a fixed time instance or rotor angle φ).

Assume further that these lengths are locally magnified to account for permeance drops under stator and rotor slots. These drops are chosen in such a way that the total permeance over one tooth pitch coincides with the one resulting from Carter's coefficient.

Altogether, for each separate time instant, we know the function $\lambda(x)$ expressing reciprocals of the lengths of the magnetic lines in the air gap, accounting for eccentricities, slotting and bearings' damage.

Based on the general definition of the mutual inductance:

$$L_{1,2} = \frac{\psi_{1(2)}}{i_2}, \tag{16}$$

one achieves the following formula for mutual inductance, in the case of an induction machine:

$$L_{12} = z_1 z_2 (\Lambda_{12} - \frac{\Lambda_1 \Lambda_2}{\Lambda_u}), \tag{17}$$

where:

$$\Lambda_i = \mu_0 r l \int\limits_{(x_{bi}, x_{ei})} \lambda(x) dx, \quad \text{for } i = 1, 2 \tag{18}$$

$$\Lambda_{12} = \mu_0 r l \int\limits_{(x_{b1}, x_{e1}) \cap (x_{b2}, x_{e2})} \lambda(x) dx, \tag{19}$$

$$\Lambda_u = \mu_0 r l \int\limits_{(0, 2\pi)} \lambda(x) dx + \Lambda_{ends}, \tag{20}$$

– r, l – middle air-gap radius and axial length;
– Λ_{ends} – permeance for the axial-flux leak (omitted in calculations).

The range of integration in (18) is (x_{bi}, x_{ei}), that is from the left to the right side of the coil considered (numbered as 1 or 2).

The range of integration in (19) is (x_{b1}, x_{e1})$\cap$(x_{b1}, x_{e1}). It is the union of the ranges from (18).

The range of integration in (20) is full: (0,2π).

The coils 1 and 2 can be thought to be placed on the stator or rotor, as the lines of the main magnetic flux are assumed to cross the air gap down the straight paths. These paths are radial only by lack of eccentricities.

Once the formulas (17) to (20) are established, calculations of machine's inductances is a matter of implementing an appropriate program. In program implementation the integrals (18) to (20) are calculated in a numerical way. Formula (17) is used for all the stator and rotor elementary coils. The calculated main inductances are then accomplished by leakage inductances calculated in a classical way, whereby they are assumed to be constant.

The thus established self- and mutual inductances (of single stator coils and cage meshes) are transformed via a stator connection matrix C.

At this stage all the self- and mutual inductances (of all the linearly independent circuits) are calculated for just one single rotor position and the values are stored in a 2D matrix on disc.

These calculations are repeated for as many as about 400 rotor positions. Hence, one obtains a 3D matrix of inductances and their derivatives on the disc.

3. Numerical Calculations

Fig. 1. shows spectra of stator currents for various degrees of vibration of the rotor, similar to those resulting from a damaged bearing. The rotor vibration degree is understood as rotor vibration amplitude expressed as percentage of the air-gap length. It is referred to as "runOut' in Figs 1 through 5. The calculations were made for a 1.1 kW, three phase motor with 24 stator and 22 rotor slots. They were performed for a number of radial rotor vibrations, oscillating eight times faster than the actual rotational speed of the rotor. This means that in the calculations it has been assumed that additional vibrations of the position of the rotor's axis depend on $8 \cdot \varphi$ where φ is the angle of rotation of the rotor.

The values of spectral lines carrying information on the motor's vibrations appear in the interval from – 60 to – 100 dB with respect to the fundamental component F1 with a frequency of 50 Hz, designated with the number 1 in Fig.1. The harmonic F13, numbered 13, is the slot harmonic. Its frequency is F13 = 1098.6 Hz. This frequency is related to the slip s through the relation [4]:

$$f_S = f_1 + h \cdot N_R \cdot (1 - s) \cdot 50 / p. \tag{21}$$

where f_1 = 50 Hz, N_R = 22, and a number of pole pairs p=2.

This motor belongs to the category "210" with the parameter h=2. From [3] it results that the slip is 0.04672. This corresponds to a rotational speed n=23.83 rps. The rotor oscillation frequency is $f_w = 8 \cdot n = 190.64$ Hz. Double frequency of vibrations is $D = 2 \cdot 190.64 = 381.28$ Hz.

Thus in the spectra in Fig. 1 we find the following frequencies:

F5 = 50 + D [Hz];

F9 = 50 + 2·D [Hz];

F4 = |50-D| = D – 50 [Hz];

F8 (the one on the left) = |50-2·D| = 2·D – 50 [Hz].

Also the slot harmonic F13 gives rise to its own chain of harmonics caused by rotor vibrations:

F14 = F13 + D [Hz];

F8 (the one on the right, barely visible) = F13 – D [Hz].

Harmonic F6 appearing with a centric rotor (without radial vibrations) is the source of harmonics F2 and F10:

F2 = F6 – D [Hz];

F10 = F6 + D [Hz].

Harmonic F7 appearing with a centric rotor (without radial vibrations) is the source of harmonics F3 and F11:

F3 = F7 – D [Hz];

F11 = F7 + D [Hz].

Generally, the following conclusions can be drawn from tests performed on a model:

1. All frequency components present in the spectrum of a motor with a centric rotor can be modulated with a frequency of $2 \cdot f_w$ (and its multiples), where f_w is the frequency of oscillations of the air gap
2. The amplitudes of information-carrying spectrum components appear in the range from -60 to -90 decibels with respect to the fundamental frequency of 50 Hz.

These conclusions are important for the design and construction of a diagnostic system.

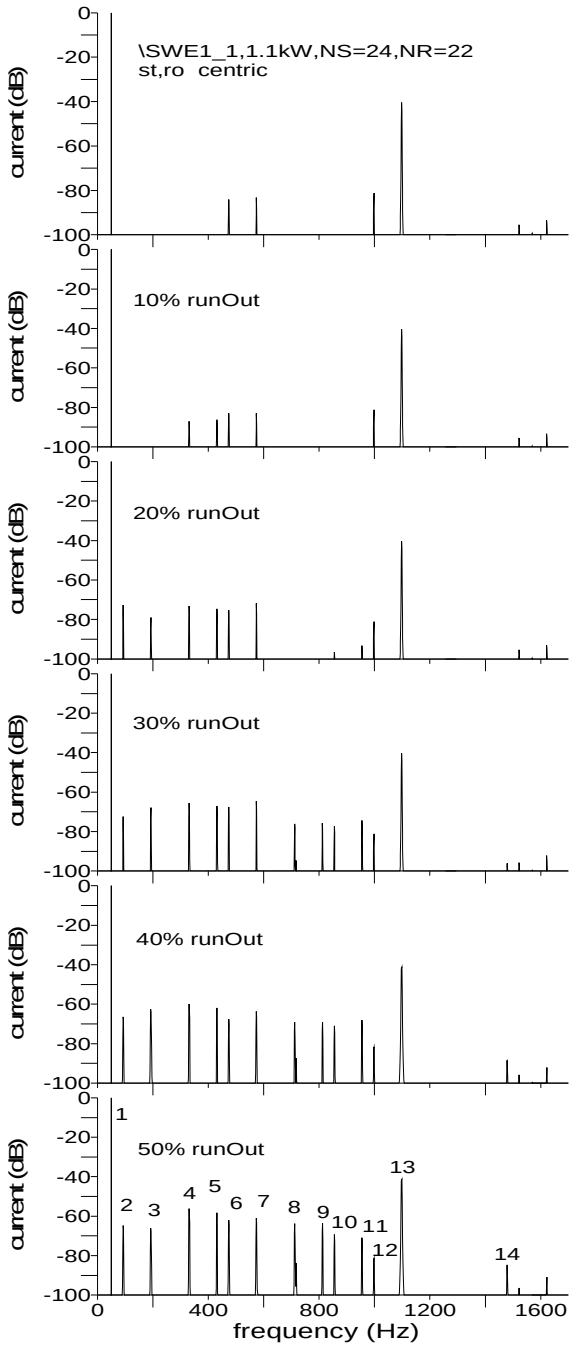

Fig. 1. Stator current harmonics (in decibels referred to a 50 Hz harmonic) for $8 \cdot \varphi$ vibrations of the rotor, for zero to 50% of the air gap length (thickness).

4. Laboratory Simulation and Measurements

Measurements and the spectrum analysis were performed in a specially developed measurement system characterized by low noise and a high dynamic range of 90 dB.

In the first stage of experimental tests it has been decided, to just facilitate the existing relations, to force the motor to the oscillations of the air gap at one specific frequency, which could have been adjusted. To achieve this, a direct-current motor with variable rotational speed has been attached to the body of the tested, elastically founded motor. The rotor of the DC motor had a specially-added eccentric mass which during rotation brought the frames of both motors into oscillation with an adjustable frequency.

The object under test was a 1.1 kW motor with two pole pairs (synchronous speed n_s=25 rps).

Fig. 2. presents the spectrum of the tested motor operating with a load of 70% of I_n without external vibration.

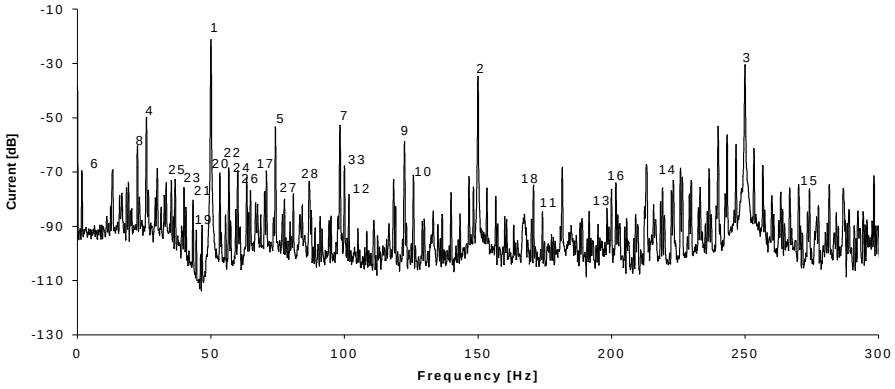

Fig. 2. The spectrum of an induction motor loaded to 70% In, without external vibrations.

Notice in Fig. 2. the appearance of the fundamental component f_1 and its odd harmonics: $3f_1$, $5f_1$. The source of the higher harmonics is the distorted supply voltage. The spectrum contains also harmonics caused by modulation of current components, resulting from distorted voltage, by the revolution frequency of the rotor. The frequencies identified in the current spectrum in Fig. 2 are summarized in Table 1.

Symbols in Table 1 are as follows: f_1 – frequency of the supply source, f_r – current rotational speed of the rotor of the tested motor, p – number of pole pairs, $df = f_1/p - f_r$.

In order to confirm the correctness of identification of the spectrum components, tests were performed at different loads of the motor. With increased loading the angular frequency is reduced and the identified components change according to relations listed in Table 1.

Fig. 3 presents the supply current spectrum of the motor for the case of an active vibrator generating oscillations with a frequency of 40 Hz. The motor under test is without load.

Crosses denote spectral lines, of no diagnostic significance, due to their presence also in the case of lack of vibrations. The other components were identified in accordance with the principle stated in Section 2 – these are the effects of modulation of the components from Table 1 with a frequency of $\pm 2 \cdot f_w$. New diagnostic components appeared, which are due to the effect of modulation of spectrum components with a single frequency f_w.

Table 1. Frequencies identified in the motor spectra in Fig. 2.

Symbol in Fig. 2	Relationship
1	f_1
2	$3f_1$
3	$5f_1$
4	$f_1 – f_r$
5	$f_1 + f_r$
6	$f_1 – 2f_r$
7	$f_1 + 2f_r$
8	$\|f_1 – 3f_r\|$
9	$f_1 + 3f_r$
10	$3f_1 - f_r$
11	$3f_1 + f_r$
12	$3f_1 – 2f_r$
13	$3f_1 + 2f_r$
14	$5f_1 – f_r$
15	$5f_1 + f_r$
16	$5f_1 – 2f_r$
17	$\|f_1 – 5f_r\|$
18	$f_1 + 5f_r$
19	f_1 –4df
20	f_1 + 4df
21	f_1 – 8df
22	f_1 + 8df
23	f_1 – 12df
24	f_1 + 12 df
25	f_1 – 16df
26	f_1 + 16df
27	f_1 – 20df
28	f_1 + 20df
29	f_1 – 24df
30	f_1 + 24df
31	f_1 – 44df
32	f_1 + 44df
33	$2f_1$
34	$2f_1$+22df
35	$3f_1 – 3f_r$

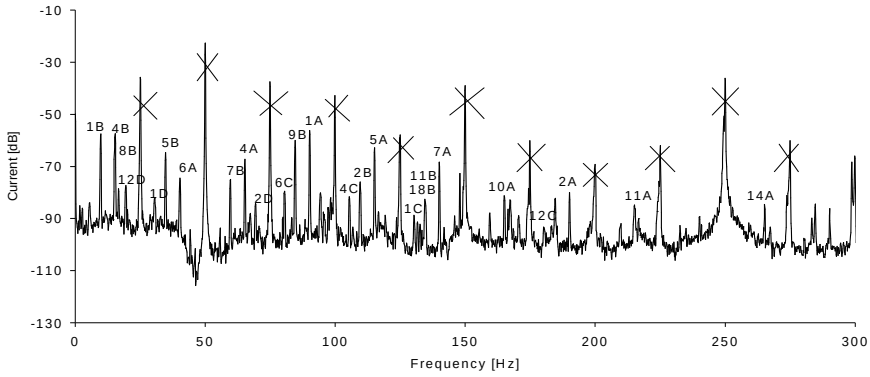

Fig. 3. The current spectrum of an idle-running induction motor with an active vibrator generating vibrations of the body of the motor under test with a frequency of 40 Hz.

An example of notations used in Fig. 3: Symbol 6A in Fig. 3 denotes the modulation of the component with no.6 in Table 1 by frequency $+f_w$ (the letter B would accordingly denote the modulating frequency $-f_w$, the letter C the frequency $+2 \cdot f_w$ and the letter D the frequency $-2 \cdot f_w$).

In order to confirm the correctness of identification of the spectrum components, tests were performed at different frequencies of the vibrator. The result is shown in Fig. 4. With increased vibrator frequency the identified components change according to relations listed in Table 1.

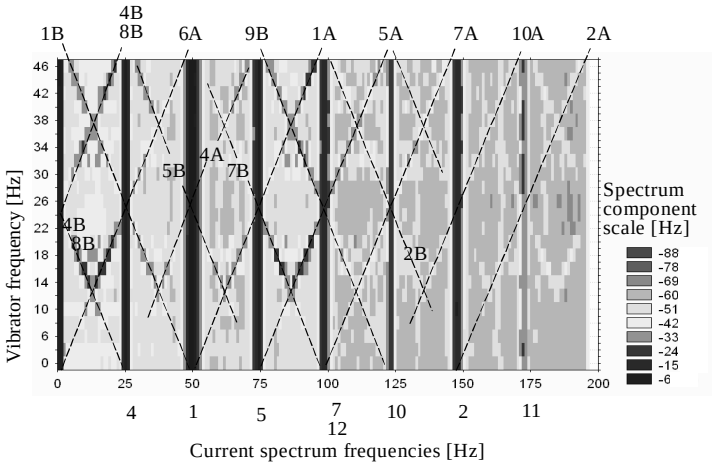

Fig. 4. The dependence between frequencies of spectrum current components and vibration frequency (numbers of components according to Table 1).

Conclusions drawn from the simulation tests are the following:

1. In the spectrum of a motor without oscillations of the air gap, components appear at harmonic frequencies of the supply voltage. There are also harmonics present which result from modulation of current components resulting from distorted voltage, by the rotational frequency,
2. In the presence of oscillations of the air gap, new components appear in the current spectrum which can be identified as products of modulation of the components described in Table 1 by the air gap oscillation frequency and its multiples.

5. Conclusion

1. Diagnostics of bearings, based on the analysis of the current spectrum becomes easier when the motor runs idle – the spectrum contains more diagnostic components with greater amplitudes.
2. The assumption of a general thesis that all frequency components present in the spectrum of a motor with eccentric rotor can be modulated by the $\pm f_w$ and $\pm 2f_w$ frequency, where f_w is the frequency of oscillation of the air gap, permits to reduce the diagnostics to search for spectrum components with frequencies determined beforehand. The f_w frequencies for various types of bearing faults are given in [1].
3. Success requires that the measurement system have an accordingly low noise level and high dynamic range of measurement.
4. The measurement of the angular velocity and of the supply network frequency should be carried out and averaged over the same time interval in which the current signal sample

has been taken for spectrum analysis.

5. Due to the fact that generally the current spectrum contains a number of components with closely spaced frequencies, it is necessary to determine the frequency of the supply network as well as the rotational frequency with an inaccuracy not exceeding ± 0.03 Hz. It is also necessary to have a spectrum resolution of at least 1/8 Hz.

References

[1] R.R. Schoen, T.G. Habetler, F. Karman, R.G. Bartheld: "Motor bearing damage detection using stator current monitoring". *IEEE Transactions on Industry Applications*, vol. 31, no. 6, Nov/Dec 1995, pp. 1274-1279.

[2] B. Yazici, G.B. Kliman: "An adaptive statistical time-frequency method for detection of broken bars and bearing faults in motors using stator current". *IEEE Transactions on Industry Applications*, vol. 35, no. 2, March/April 1999, pp.442-452.

[3] J. Rusek: "Computer implementation of the induction machine dynamical model accounting for broken bars, eccentricities, slotting and parallel branches". *Proc. ICEM 2000 Conference*, Espo, Finland 2000, pp.868-872.

[4] J. Rusek: "Categorization of Induction Machines Resulting from Their Harmonic-Balance Model". *Electromagnetics*, no. 23, 2003, pp. 277-292.